

## Supporting Information

for *Adv. Funct. Mater.*, DOI: 10.1002/adfm.202207763

Hierarchically Assembled Counter Electrode for Fiber  
Solar Cell Showing Record Power Conversion Efficiency

*Xinyue Kang, Zhengfeng Zhu, Tiancheng Zhao,  
Weijie Zhai, Jianchen Xu, Zhengmeng Lin, Kaiwen  
Zeng, Bingjie Wang, Xuemei Sun, Peining Chen,\* and  
Huisheng Peng\**

## Supporting Information

### **Hierarchically Assembled Counter Electrode for Fiber Solar Cell Showing Record Power Conversion Efficiency**

*Xinyue Kang<sup>†</sup>, Zhengfeng Zhu<sup>†</sup>, Tiancheng Zhao, Weijie Zhai, Jianchen Xu, Zhengmeng Lin, Kaiwen Zeng, Bingjie Wang, Xuemei Sun, Peining Chen\* and Huisheng Peng\**

*X. Kang, Dr. Z. Zhu, T. Zhao, W. Zhai, J. Xu, Z. Lin, Dr. K. Zeng, Prof. B. Wang, Prof. X. Sun, Prof. P. Chen, Prof. H. Peng*

*State Key Laboratory of Molecular Engineering of Polymers, Department of Macromolecular Science and Laboratory of Advanced Materials, Fudan University, Shanghai 200438, China, E-mail: peiningc@fudan.edu.cn; penghs@fudan.edu.cn.*

*<sup>†</sup>The first two authors contributed equally to this work.*

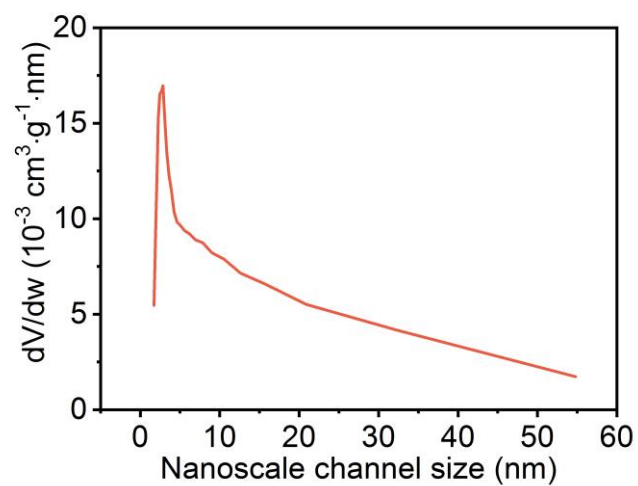


**Figure S1.** N<sub>2</sub> absorption-desorption isotherms of CNT.



**Figure S2.** Photograph of reels of primary CNT fibers.

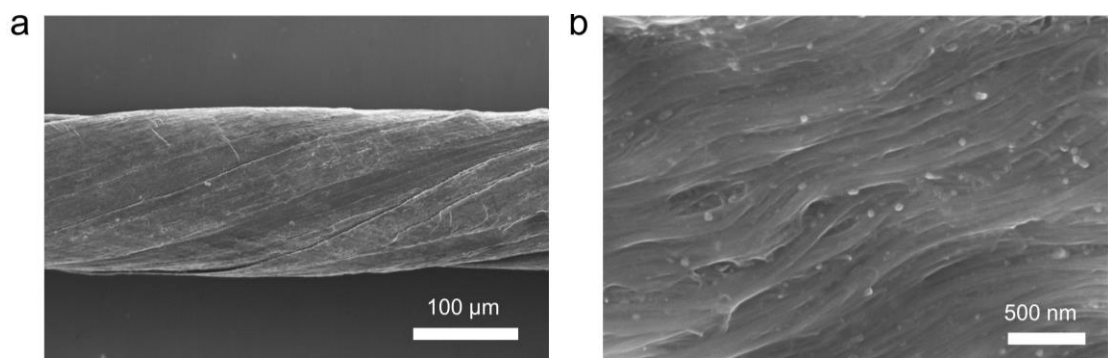


**Figure S3.** SEM image of CNT fiber (with diameter of  $\sim 150 \mu\text{m}$ ) at low (a) and high (b) magnifications.

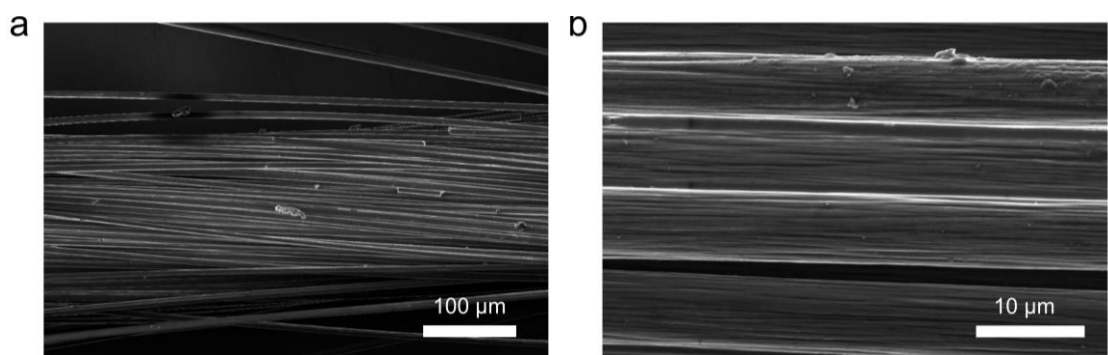


**Figure S4.** SEM image of carbon fiber (with diameter of  $\sim 150 \mu\text{m}$ ) at low (a) and high (b) magnifications.

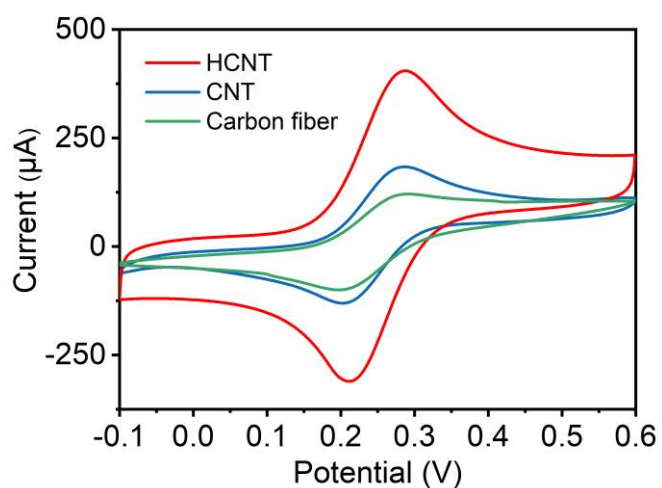


**Figure S5.** CV curves of electrochemical activity area measurement in the 20 mM  $\text{K}_4\text{Fe}(\text{CN})_6$  and 0.2 M KCl at  $20 \text{ mV}\cdot\text{s}^{-1}$ .

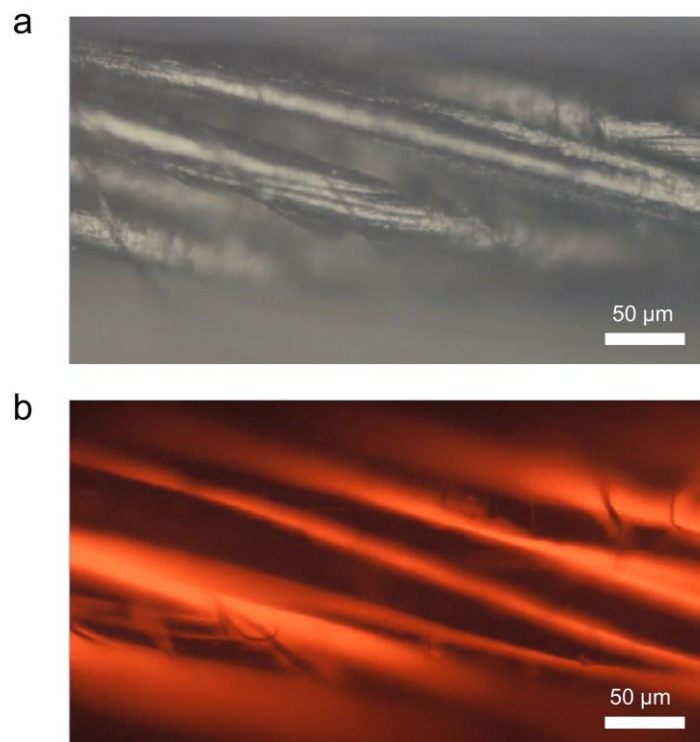


**Figure S6.** Optical (a) and fluorescence (b) micrographs of HCNT fiber with ethanol solution containing rhodamine indicate that the electrolyte infiltrated into microchannels.

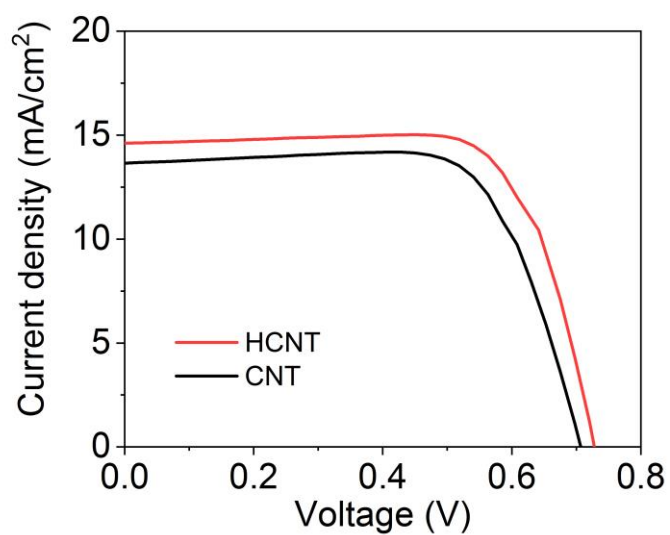


**Figure S7.** *J-V* curves of N719-sensitized fiber solar cells (with I<sup>-</sup>/I<sub>3</sub><sup>-</sup> electrolyte) using HCNT and CNT fibers as counter electrodes.

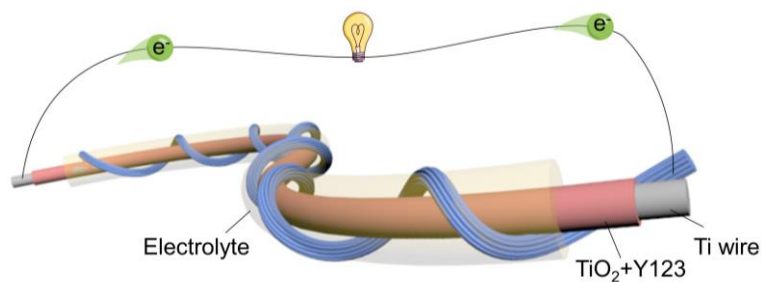


**Figure S8.** Structure of FDSSC and flow direction of electrons in external circuit.

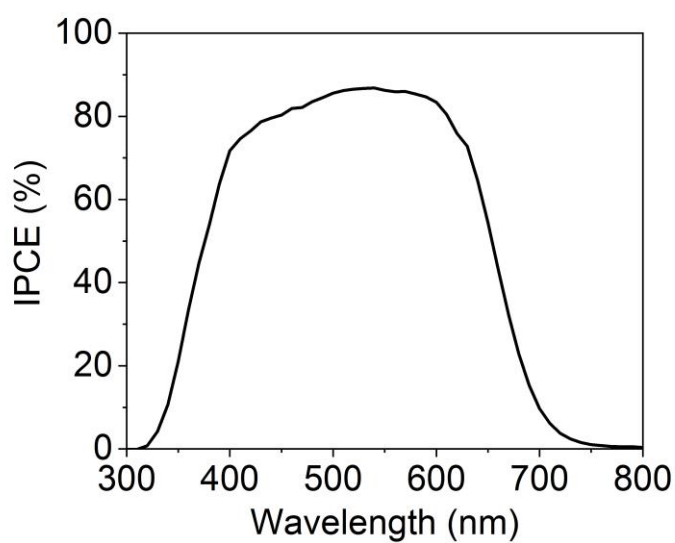


**Figure S9.** IPCE spectra of HCNT@Pt-based FDSSC.

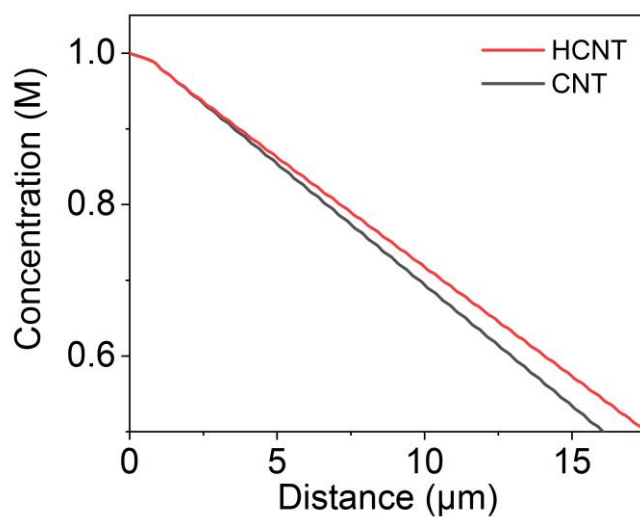


**Figure S10.** The curves of simulated ion concentration inside the fiber electrodes along the distance from electrodes surface. The simulation was performed by COMSOL Multiphysics 6.0. The initial concentration of  $\text{Co}^{3+}$  was 1 M. The diffusion coefficient was  $1 \times 10^{-10} \text{ m}^2/\text{s}$ .

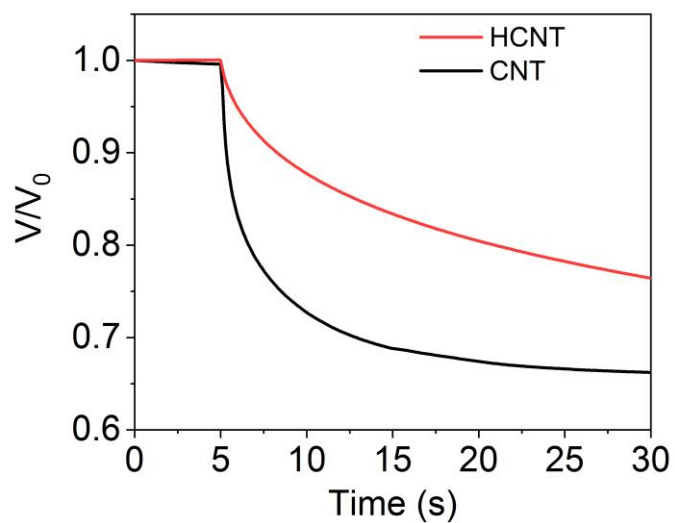


**Figure S11.** The open-circuit voltage decay curves of HCNT-based and CNT-based FDSSCs.

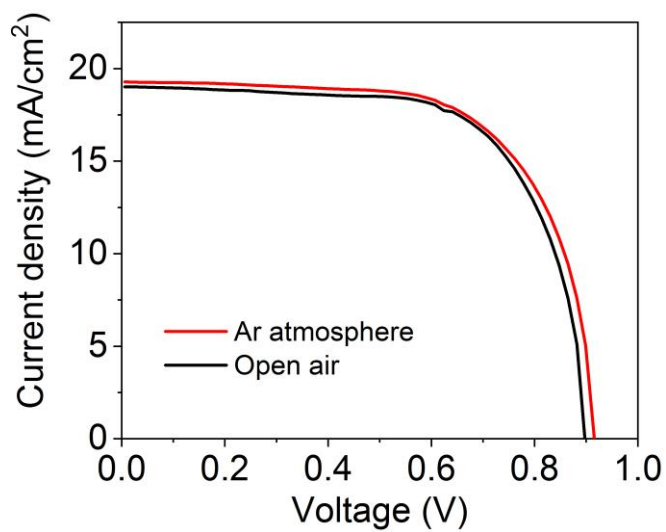


**Figure S12.**  $J$ - $V$  curves of the FDSSCs measured under Ar atmosphere and open air conditions.

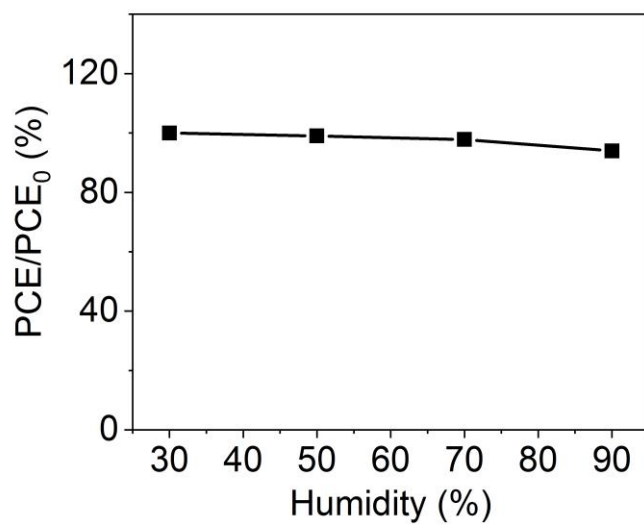


**Figure S13.** Variations of PCEs for FDSSCs under different humidity levels.

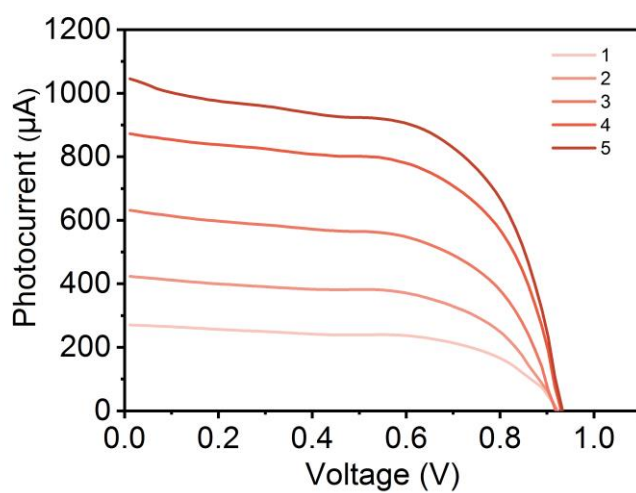


**Figure S14.**  $I$ - $V$  curves of the fabric modules with increasing numbers of FDSSCs connected in parallel.



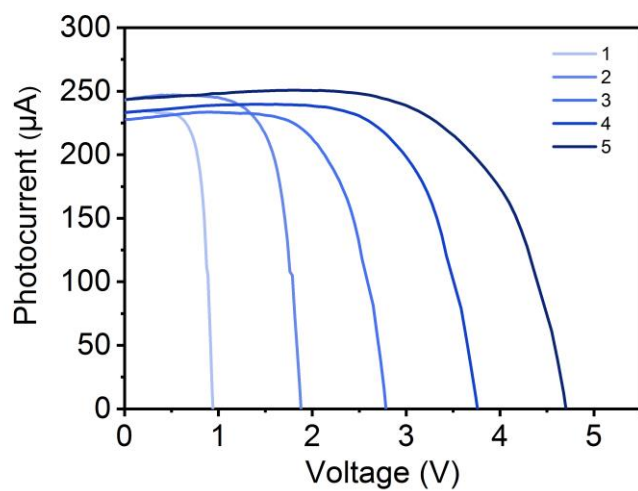


**Figure S15.**  $I$ - $V$  curves of the fabric modules with increasing numbers of FDSSCs connected in series.

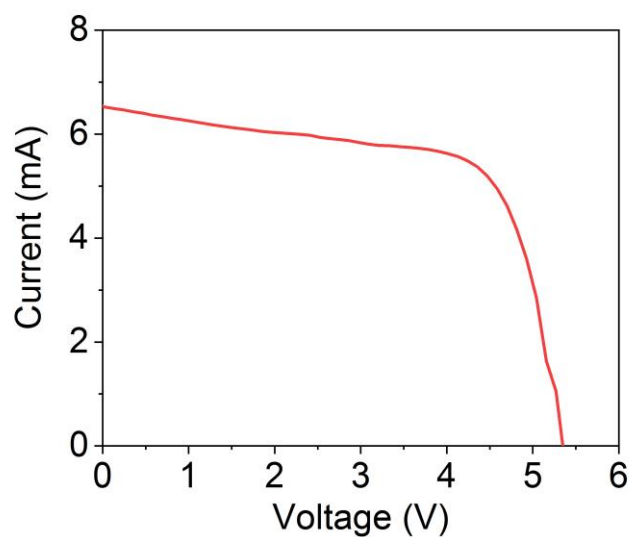


**Figure S16.** The  $J$ - $V$  curve of the photovoltaic textile measured under the illumination of AM 1.5G.

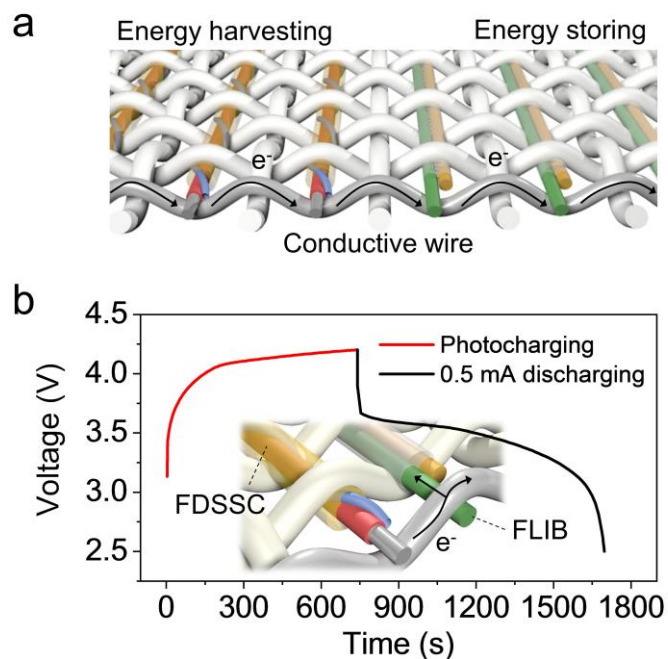


**Figure S17.** (a) Scheme to a textile woven by FDSSCs and FLIBs. (b) Photocharging curve of FDSSCs under AM 1.5 (red line) and discharging curve at 0.5 mA (black line) of the FLIB. Inset: operating mechanism of electron flow along conducting wire from the photoanode to the negative electrode.

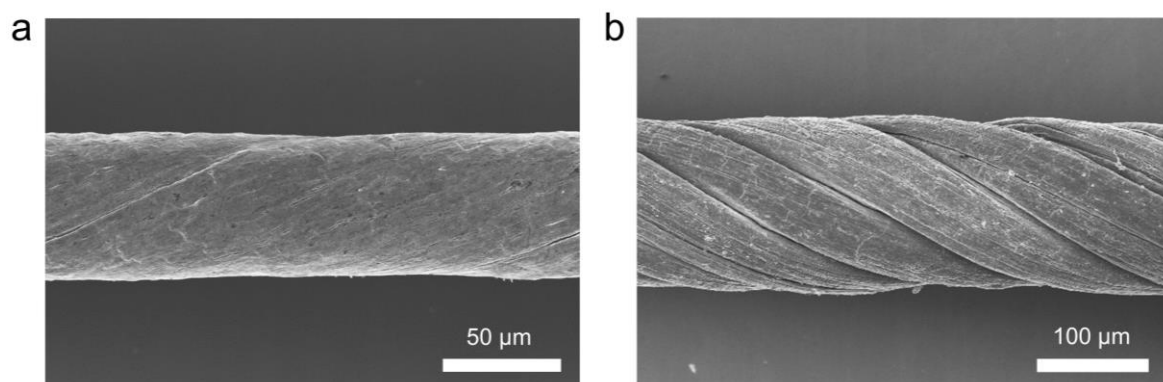


**Figure S18.** (a) SEM image of primary CNT fiber with diameter of 60 μm. (b) SEM image of HCNT-1 fiber with diameter of 150 μm.

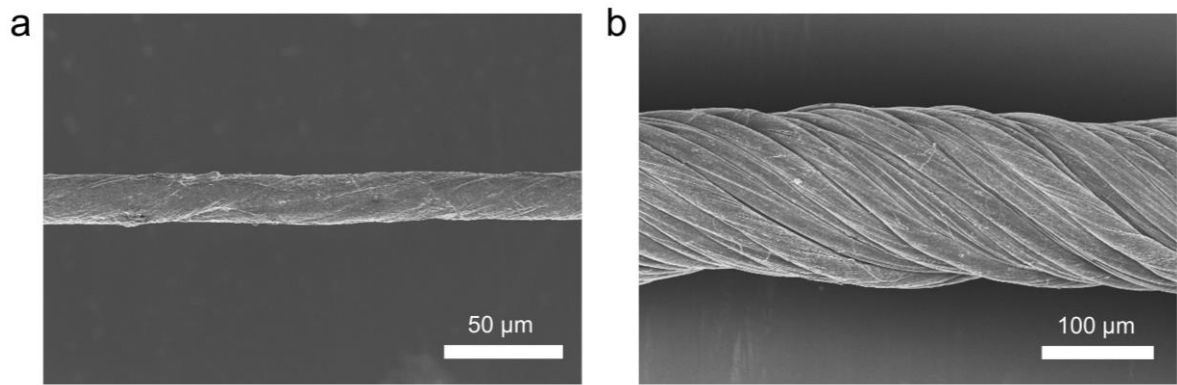


**Figure S19.** (a) SEM image of primary CNT fiber with diameter of 20  $\mu\text{m}$ . (b) SEM image of HCNT-3 fiber with diameter of 150  $\mu\text{m}$ .

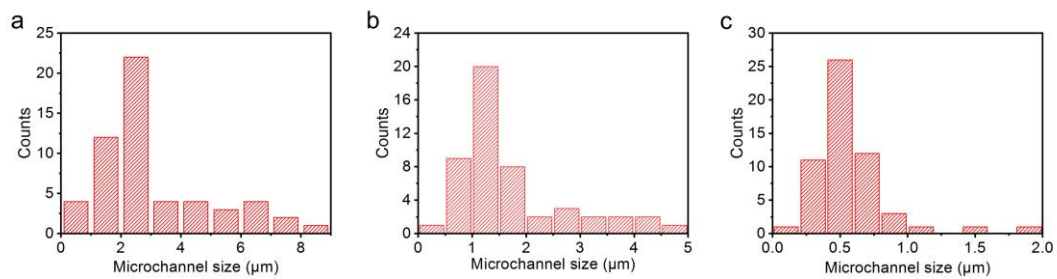


**Figure S20.** Statistical distribution of the channel size for microchannels in HCNT-1 fiber (average size of  $3 \pm 1.97 \mu\text{m}$ ) (a), HCNT-2 fiber (average size of  $1.7 \pm 1.01 \mu\text{m}$ ) (b), and HCNT-3 fiber (average size of  $0.5 \pm 0.29 \mu\text{m}$ ) (c). The sample number was 50 for each statistical analysis.

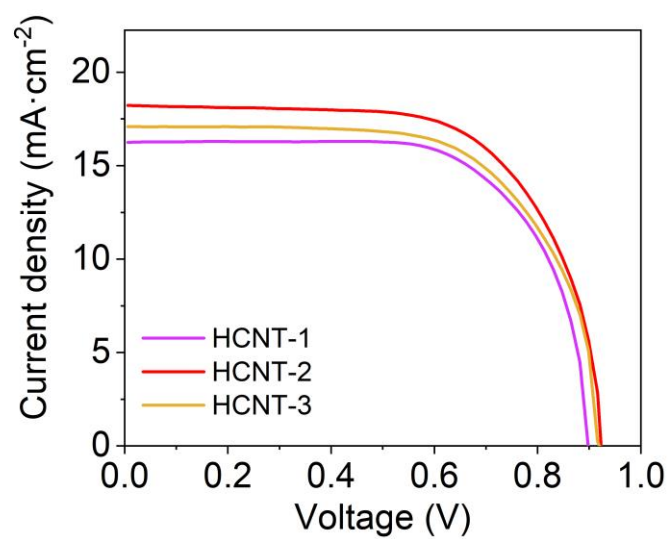


**Figure S21.**  $J$ - $V$  curves of the FDSSCs using different counter electrodes.

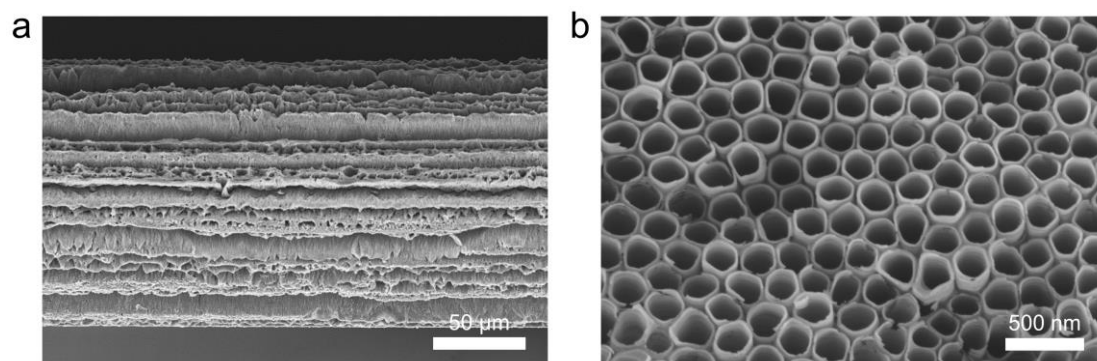


**Figure S22.** SEM images of fiber photoanode at (a) low and (b) high resolution.

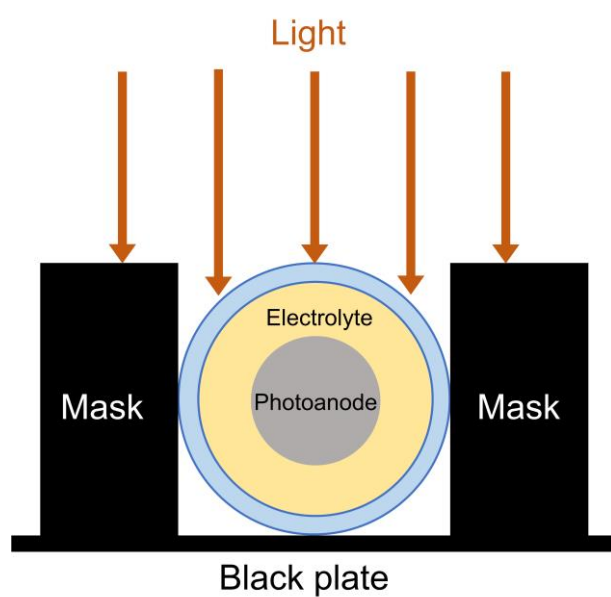


**Figure S23.** The schematic illustration of  $J$ - $V$  measurement.

**Table S1.** EIS data in Figure 3c.

	$R_s/(\Omega \cdot \text{cm}^2)$	$R_{ct}/(\Omega \cdot \text{cm}^2)$	$Z_N/(\Omega \cdot \text{cm}^2)$
<b>Carbon fiber</b>	43.3	6.57	150.9
<b>CNT fiber</b>	7.9	0.44	141.4
<b>HCNT fiber</b>	6.7	0.38	84.3

**Table S2.** Photovoltaic parameters of the FDSSCs in Figure 3d.

	$V_{oc}/(\text{V})$	$J_{sc}/(\text{mA} \cdot \text{cm}^{-2})$	<b>FF</b>	<b>PCE/(%)</b>
<b>Carbon fiber</b>	0.773	11.14	0.63	5.43
<b>CNT fiber</b>	0.889	15.11	0.66	8.89
<b>HCNT fiber</b>	0.923	18.26	0.66	11.14
<b>HCNT@Pt fiber</b>	0.907	19.32	0.68	11.94

**Table S3.** Photovoltaic parameters of the FDSSCs with different Pt loadings.

<b>Pt loadings/(mg/cm<sup>2</sup>)</b>	$V_{oc}/(\text{V})$	$J_{sc}/(\text{mA}/\text{cm}^2)$	<b>FF</b>	<b>PCE/(%)</b>
2.12	0.870	19.09	0.68	11.28
4.24	0.907	19.32	0.68	11.94
8.48	0.907	19.05	0.68	11.82

**Table S4.** Comparison of PCEs for fiber solar cells to date.

<b>PVs Type</b>	<b>Cathode</b>	<b>Anode</b>	<b>PCE (%)</b>	<b>Reference</b>
<b>DSSC</b>	HS-CNT fiber	Ti-TiO <sub>2</sub> NT	11.94	This work
	Graphene fiber/Pt	Ti-TiO <sub>2</sub> NT	8.45	[1]
	RGO/CNT fiber/Pt	Ti-TiO <sub>2</sub> NT	8.50	[2]
	Pt wire	Multiple Ti-TiO <sub>2</sub> NT	9.1	[3]
	Pt wire	Ti-TiO <sub>2</sub> film-TiO <sub>2</sub> NP	7.41	[4]
	CF@TiO <sub>2</sub> @MoS <sub>2</sub>	Ti-TiO <sub>2</sub> NT	9.5	[5]
	Pt/CS-CNT fiber	Ti-TiO <sub>2</sub> NT	10.00	[6]
	CF@PANI@CoSe	Ti-TiO <sub>2</sub> NT	10.28	[7]
	Pt wire	Ti-TiO <sub>2</sub> @PEO <sub>x</sub>	11.22	[8]
<b>OSC</b>	PEDOT:PSS	SS-ZnO	2.3	[9]
	PEDOT:PSS	SS-ZnO	2.53	[10]
	PEDOT:PSS	Ti-TiO <sub>2</sub> NP	1.78	[11]
	PEDOT:PSS	Ti-TiO <sub>2</sub> NT	1.23	[12]
	PEDOT:PSS	Ti-ZnO	1.62	[13]
	PEDOT:PSS	Graphene-ZnO	2.13	[14]
<b>PSC</b>	OMeTAD	SS- TiO <sub>2</sub> NP	3.3	[15]
	Spiro-OMeTAD	Ti-TiO <sub>2</sub> NT	5.22	[16]
	CNT	PEN-TiO <sub>2</sub>	9.49	[17]
	Spiro-OMeTAD	Ti-TiO <sub>2</sub> NP	6.58	[18]
	Spiro-OMeTAD	Ti-TiO <sub>2</sub> NP	7.53	[19]
	Spiro-OMeTAD	Ti-TiO <sub>2</sub> NP	10.79	[20]
	P3HT	ETL free	7.49	[21]

**Table S5.** The acetonitrile infiltration time for different fiber electrodes.

Number of sample	Infiltration time for CNT fibers (s)	Infiltration time for HCNT fibers (s)
1	45	19
2	35	21
3	48	27
Average	42.7	22.3

## References

- [1] Z. Yang, H. Sun, T. Chen, L. Qiu, Y. Luo, H. Peng, *Angew. Chem. Int. Ed.* **2013**, 52, 7545-7548.
- [2] H. Sun, X. You, J. Deng, X. Chen, Z. Yang, J. Ren, H. Peng, *Adv. Mater.* **2014**, 26, 2868-2873.
- [3] J. Liang, G. Zhang, W. Sun, P. Dong, *Nano Energy* **2015**, 12, 501-509.
- [4] W. Song, H. Wang, G. Liu, M. Peng, D. Zou, *Nano Energy* **2016**, 19, 1-7.
- [5] J. Liang, G. Zhu, C. Wang, Y. Wang, H. Zhu, Y. Hu, H. Lv, R. Chen, L. Ma, T. Chen, Z. Jin, J. Liu, *Adv. Energy Mater.* **2017**, 7, 1601208.
- [6] X. Fu, H. Sun, S. Xie, J. Zhang, Z. Pan, M. Liao, L. Xu, Z. Li, B. Wang, X. Sun, H. Peng, *J. Mater. Chem. A* **2018**, 6, 45-51.
- [7] J. Zhang, Z. Wang, X. Li, J. Yang, C. Song, Y. Li, J. Cheng, Q. Guan, B. Wang, *ACS Appl. Energy Mater.* **2019**, 2, 2870-2877.
- [8] R. E. A. Ardhi, M. X. Tran, M. Wang, G. Liu, J. K. Lee, *J. Mater. Chem. A* **2020**, 8, 2549-2562.
- [9] D. Y. Liu, M. Y. Zhao, Y. Li, Z. Q. Bian, L. H. Zhang, Y. Y. Shang, X. Y. Xia, S. Zhang, D. Q. Yun, Z. W. Liu, A. Y. Cao, C. H. Huang, *ACS Nano* **2012**, 6, 11027-11034.
- [10] D. Liu, Y. Li, S. Zhao, A. Cao, C. Zhang, Z. Liu, Z. Bian, Z. Liu, C. Huang, *RSC Adv.* **2013**, 3, 13720-13727.
- [11] Z. Zhang, Z. Yang, Z. Wu, G. Guan, S. Pan, Y. Zhang, H. Li, J. Deng, B. Sun, H. Peng, *Adv. Energy Mater.* **2014**, 4, 1301750.
- [12] Z. Zhang, Z. Yang, J. Deng, Y. Zhang, G. Guan, H. Peng, *Small* **2015**, 11, 675-680.
- [13] P. Liu, Z. Gao, L. Xu, X. Shi, X. Fu, K. Li, B. Zhang, X. Sun, H. Peng, *J. Mater. Chem. A* **2018**, 6, 19947-19953.

- [14] M. Hilal, J. I. Han, *Electrochim. Acta* **2019**, 326, 134985.
- [15] L. Qiu, J. Deng, X. Lu, Z. Yang, H. Peng, *Angew. Chem. Int. Ed.* **2014**, 53, 10425-10428.
- [16] J. Deng, L. Qiu, X. Lu, Z. Yang, G. Guan, Z. Zhang, H. Peng, *J. Mater. Chem. A* **2015**, 3, 21070-21076.
- [17] L. Qiu, S. He, J. Yang, F. Jin, J. Deng, H. Sun, X. Cheng, G. Guan, X. Sun, H. Zhao, H. Peng, *J. Mater. Chem. A* **2016**, 4, 10105-10109.
- [18] B. Chen, S. Chen, B. Dong, X. Gao, X. Xiao, J. Zhou, J. Hu, S. Tang, K. Yan, H. Hu, K. Sun, W. Wen, Z. Zhao, D. Zou, *Adv. Mater. Interfaces* **2017**, 4, 1700833.
- [19] H. Hu, B. Dong, B. Chen, X. Gao, D. Zou, *Sustain. Energy Fuels* **2018**, 2, 79-84.
- [20] B. Dong, J. Hu, X. Xiao, S. Tang, X. Gao, Z. Peng, D. Zou, *Adv. Mater. Technol.* **2019**, 4, 1900131.
- [21] A. Balilonda, Q. Li, X. Bian, R. Jose, S. Ramakrishna, M. Zhu, F. Zabihi, S. Yang, *Chem. Eng. J.* **2021**, 410, 128384.